

Partial oxidation of methane using Pt/CeZrO₂/Al₂O₃ catalysts – effect of preparation methods

Priscila P. Silva^a, Fabiano A. Silva^a, Helena P. Souza^b, Adriane G. Lobo^b,
Lisiane V. Mattos^b, Fábio B. Noronha^{b,1}, Carla E. Hori^{a,*}

^a Faculdade de Engenharia Química, Universidade Federal Uberlândia, Av. João Naves de Ávila, 2160,
Bloco 1K, Campus Santa Mônica, CEP 38400-902 Uberlândia, MG, Brazil

^b Instituto Nacional de Tecnologia (INT), Av. Venezuela 82, CEP 20081-312 Rio de Janeiro, RJ, Brazil

Available online 2 March 2005

Abstract

The effect of the preparation method of Pt/CeZrO₂/Al₂O₃ catalysts on the dispersions of the metal and of the ceria–zirconia on the surface of the alumina and on the catalytic performance of methane partial oxidation reaction was evaluated. The ceria–zirconia materials were supported on the alumina surface by precipitation and impregnation and all the samples contained 1.5 wt.% of Pt. The dispersion of the ceria–zirconia was evaluated by adsorbed CO₂ infrared spectroscopy and the dispersion of the metal was determined by the dehydrogenation of cyclohexane. The reducibility of the catalysts was measured by oxygen storage capacity and temperature programmed reduction. The samples prepared by impregnation present higher activity, stability and selectivity to form CO and H₂ than the ones prepared by precipitation. The characterization results show that all the samples had practically the same platinum dispersion but the dispersion of the ceria–zirconia material on the alumina was more effective when the impregnation method was used. The impregnation favors a high coverage degree of the alumina by the ceria-based oxides. This means that a larger fraction of platinum particles is in contact with ceria or ceria–zirconia oxide. The metal–support interface is a key factor to avoid the carbon deposits that are responsible for the deactivation of some samples.

© 2004 Elsevier B.V. All rights reserved.

Keywords: Partial oxidation of methane; Pt/Ce–ZrO₂/Al₂O₃ catalysts; Oxygen storage capacity; Ceria; Ceria–zirconia

1. Introduction

The vast majority of the known natural gas reserves are located in remote areas. The development of processes that convert natural gas into liquid fuels such as gasoline and diesel is the subject of research for several groups around the world. The most traditional route to convert natural gas into liquid fuels (gas to liquid – GTL) is to transform methane into synthesis gas, and then produce hydrocarbons using Fischer–Tropsch synthesis [1–3]. However, the generation of the synthesis gas accounts for between 50 and 75% of the total investment required [4]. Therefore, in order to make

GTL technology economically viable, it is necessary to reduce these costs.

Presently, the commercial process to obtain synthesis gas is through steam reforming. This reaction is extremely endothermic and produces a carbon monoxide to hydrogen ratio that is not adequate to GTL process [5]. The partial oxidation of methane could be an alternative route to produce synthesis gas at a lower price [1,6–10]. This reaction is moderately exothermic, produces an adequate H₂/CO ratio for the Fischer–Tropsch synthesis and if it is associated to a technology that is able to separate oxygen from air, such as selective membranes, it will be a good option to lower the production cost of synthesis gas [9,10].

The literature reports that several transition metals, such as Pt, Rh and Ru, are active for the partial oxidation of methane [11–14]. In order to have a good performance for this reaction, the catalyst must have high activity, selectivity

* Corresponding author. Fax: +55 34 3239 4188.

E-mail addresses: fabibel@int.gov.br (F.B. Noronha), cehori@ufu.br (C.E. Hori).

¹ Tel.: +55 21 2123 1177; fax: +55 21 2123 1051.

and stability since one of the biggest problems in this process is the catalyst deactivation due to coke formation [14,15]. During the search of more stable catalysts, some groups have tested ceria-based materials due to its high reducibility and oxygen transfer properties [16–19]. Recently, Mattos et al. [16] investigated Pt/CeO₂, Pt/ZrO₂ and Pt/CeZrO₂ samples for the partial oxidation of methane. They verified that the sample supported on the ceria–zirconia mixed oxide presented the best activity and stability for this reaction and the good selectivity for synthesis gas. Another significant point of this study was the importance of the Pt dispersion in the catalyst's performance. The higher the metal dispersion is, the better is the activity for the reaction. Since ceria–zirconia materials usually do not provide a very high surface area, we decided to deposit ceria and ceria–zirconia on alumina.

The literature reports some studies about supported ceria–zirconia materials [19–25], the majority of them related to automotive applications. The results indicate that, when ceria–zirconia materials are supported on alumina, the incomplete incorporation of Zr into ceria lattice may occur depending on Ce/Zr ratio and preparation method. It is not clear if simple preparation methods, such as the impregnation of alumina with cerium and zirconium precursors, can lead to the formation of a ceria–zirconia solid solution. For example, Yao et al. [22] reported that it was possible to form a solid solution using impregnation for Ce/Zr ratios up to 1. On the other hand, other authors [20,24,25] did not observe the same result for Ce_{0.50}Zr_{0.50}O₂ samples supported on alumina. However, all the authors also point out that the preparation method can be of critical importance to the oxygen transfer properties of these materials. The use of alumina in the catalysts composition can be very advantageous in terms of improving metal dispersion, maintaining high surface area and reducing costs.

Therefore, the objective of this study was to evaluate the effect of the preparation method of Pt/CeZrO₂/Al₂O₃ catalysts on the dispersions of the metal and of the ceria–zirconia on the surface of the alumina and on the catalytic performance of methane partial oxidation reaction.

2. Experimental

2.1. Catalyst preparation

The alumina (Degussa) was calcined at 1173 K for 6 h in order to stabilize its surface area. The samples were prepared with around 14 wt.% of ceria or ceria–zirconia oxides and for the ceria–zirconia materials it was used a Ce/Zr atomic ratio of 3. Two preparation methods were used to disperse the ceria-based materials on the alumina surface: precipitation (pp) and incipient wetness impregnation (imp). For the precipitation method, an aqueous solution of cerium (IV) ammonium nitrate (Aldrich) and zirconium nitrate (MEL Chemicals) was prepared and mixed with the alumina. Then, the ceria and zirconium hydroxides were co-precipitated by

the addition of an excess of ammonium hydroxide. Finally, the precipitate was washed with distilled water and calcined at 1073 K for 4 h in a muffle. For the incipient wetness impregnation method the same cerium and zirconium precursors were used. The samples were dried at 373 K for 12 h and then calcined in a muffle furnace at 1073 K for 4 h.

The addition of platinum was done by incipient wetness impregnation of the supports with an aqueous solution of H₂PtCl₆ (Aldrich) and all the samples were dried at 393 K. The catalysts were calcined under air (50 ml/min) at 773 K for 4 h. All samples contained 1.5 wt.% of platinum.

2.2. X-ray diffraction (XRD)

X-ray diffraction measurements were made using a RIGAKU diffractometer with a Cu K α radiation. After calcining the samples at 1073 K, the XRD data were collected at 0.04° per step with integration times of 1 s/step between $2\theta = 25$ and 65° . All the samples were also submitted to measurements at 0.02° per step with integration times of 1 s/step between $2\theta = 27$ and 32° .

2.3. Temperature programmed reduction (TPR)

Temperature programmed reduction (TPR) measurements were carried out in a micro-reactor coupled to a quadrupole mass spectrometer (Balzers, Omnistar). The samples (300 mg) were dehydrated at 423 K for 30 min in a He flow prior to reduction. After cooling to room temperature, a mixture of 2% H₂ in Ar flowed through the sample at 30 ml/min, raising the temperature at a heating rate of 10 K/min up to 1273 K.

2.4. Oxygen storage capacity (OSC)

Oxygen storage capacity (OSC) measurements were carried out in a micro-reactor coupled to a quadrupole mass spectrometer (Balzers, Omnistar). The samples were reduced under H₂ at 773 K for 1 h and heated to 1073 K in flowing He. Then, the samples were cooled to 723 K and a 5% O₂/He mixture was passed through the catalyst until the oxygen uptake was finished. The reactor was purged with He and the dead volume was obtained by switching the gas to the 5% O₂/He mixture. Finally the amount of oxygen consumed on the catalysts was calculated taking into account a previous calibration of the mass spectrometer.

2.5. Dehydrogenation of cyclohexane

In the literature, structure insensitive reactions have been reported in the characterization of catalysts [26–29]. In particular, structure insensitive reactions were used to determine Pt dispersions on ceria containing samples is growing since more traditional techniques such as H₂ or CO chemisorption are not recommended for these catalysts due

to the possibility of adsorption of both gases on ceria [26,27]. TEM measurements are also imprecise since there is not enough contrast between ceria and platinum particles. Accordingly to Rogemond et al. it is quite possible to use the dehydrogenation of cyclohexane to determine metal dispersions provided that a preliminary calibration is done [26]. Recently, Pantu and Gavalas [27] used the propene hydrogenation as a structure insensitive reaction to obtain Pt dispersions of Pt/CeO₂ catalysts.

Therefore, we used the dehydrogenation of cyclohexane as an insensitive structure reaction [26] in order to determine the apparent dispersion of ceria–zirconia supported Pt catalysts. The dispersions of different Pt/Al₂O₃ samples were determined by H₂ chemisorption and the rate of cyclohexane dehydrogenation was also measured for each one. With these data, it was possible to correlate the Pt dispersions with the activity for this reaction. The opposite was done for the ceria containing samples: the rate was determined and using the calibration curve, it was possible to calculate the Pt dispersions.

The reaction was performed at 10⁵ Pa in a flow micro-reactor. The sample (10 mg) was previously dried in situ under N₂ flow (30 ml/min) at 393 K during 30 min. Then, the sample was cooled to room temperature and heated in pure hydrogen flow to 733 K at a heating rate of 10 K/min. This temperature was held for 1 h. The sample was then cooled in hydrogen flow to 543 K. The reaction mixture was obtained by bubbling hydrogen through a saturator containing cyclohexane (99.9%) at 285 K (H₂/C₆H₁₂ = 13.2). The space velocity was (WHSV) 170 h⁻¹ and the reaction temperatures varied from 520 to 570 K. At these conditions, no mass transfer or equilibrium limitations were observed. The conversions were kept below 10%. The composition of effluent gas phase was measured by online gas chromatograph equipped with a thermal conductivity detector and Carbowax 20-M in a Chromosorb W column.

2.6. CO₂ infrared spectroscopy

The infrared spectra of adsorbed CO₂ were obtained using a Magna 560 – Nicolet equipment. The wafers contained approximately 20 mg of support. The samples were pretreated under high vacuum at 773 K during 1 h and then submitted to an air flow (30 ml/min) during 30 min and vacuum again for 30 min at this same temperature. Then, the sample was cooled to room temperature and a first spectrum was obtained (reference). Thus, the CO₂ adsorption (pressure = 10 Torr) was performed during 1 h. The sample was then submitted to high vacuum at room temperature during 1 h and a CO₂ adsorbed spectrum was recorded.

2.7. Reaction conditions

Reaction was performed in a quartz reactor at atmospheric pressure. The samples (0.02 g) were diluted with SiC (SiC/catalyst ratio = 2:1) to form a small catalyst bed (<3 mm in

height) in order to prevent heat transfer problems. Prior to reaction, the catalyst was reduced under H₂ at 773 K for 1 h and then heated to 1073 K under N₂. The reaction was carried out at 1073 K and WHSV = 260 h⁻¹ over all catalysts. A reactant mixture with CH₄:O₂ ratio of 2:1 was used and a flow rate of 100 ml/min. These reaction conditions were chosen in order to avoid mass and heat transfer problems [30,31]. The exit gases were analyzed using a gas chromatograph (Agilent 6890) equipped with a thermal conductivity detector and a CP-carboplot column (Chrompack).

3. Results and discussion

3.1. Characterization

Fig. 1 presents the XRD patterns of Pt/Al₂O₃ (A), Pt/CeO₂/Al₂O₃ (pp) (B), Pt/CeO₂/Al₂O₃ (imp) (C), Pt/Ce_{0.75}Zr_{0.25}O₂/Al₂O₃ (pp) (D) and Pt/Ce_{0.75}Zr_{0.25}O₂/Al₂O₃ (imp) (E) obtained using 2θ positions between 25 and 65°. The Pt/Al₂O₃ (A) diffraction pattern presented the peaks characteristics of γ-alumina. The addition of ceria lead to the appearance of new diffraction peaks that are attributed to the ceria cubic phase (JCPDS-4-0593). The peak related to this phase that had the highest intensity was detected at 2θ = 28.6° which is correspondent to the diffraction of Ce(1 1 1). The patterns relative to the samples that contain ceria–zirconia (D and E) are very similar. For both of them, there was a shift of all the peaks related to the ceria phase to higher 2θ positions. This result is consistent to several reports in the literature for both bulk ceria–zirconia [32–35] or ceria–zirconia supported on alumina studies [19–25]. According to them this shift could be an indication that Zr was introduced into ceria lattice. No isolated phases were detected on the ceria–zirconia supported samples.

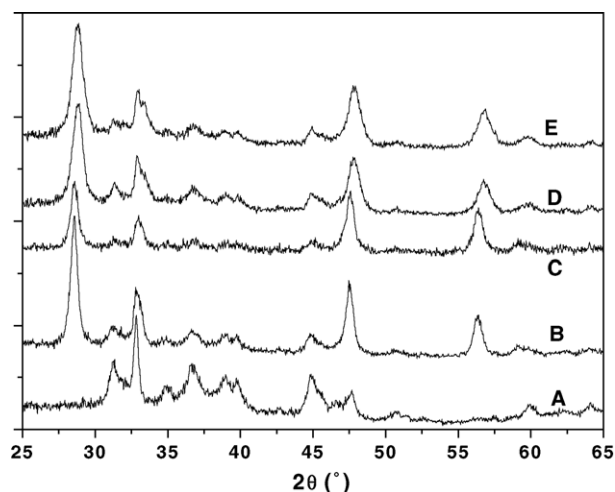


Fig. 1. X-ray diffraction patterns of Pt/Al₂O₃ (A), Pt/CeO₂/Al₂O₃ (pp) (B), Pt/CeO₂/Al₂O₃ (imp) (C), Pt/Ce_{0.75}Zr_{0.25}O₂/Al₂O₃ (pp) (D) and Pt/Ce_{0.75}Zr_{0.25}O₂/Al₂O₃ (imp) (E). Data collected at 0.04° per step between 2θ = 25 and 65°.

In order to analyze better these shifts, new X-ray diffraction data were collected using 2θ between 27 and 32° with a lower scanning speed (Fig. 2). Pt/ Al_2O_3 (A) presented only a peak at $2\theta = 32.2^\circ$ attributed to the alumina phase. Pt/ $\text{CeO}_2/\text{Al}_2\text{O}_3$ (pp) (B) had, besides this same peak at $2\theta = 32.2^\circ$, another one at $2\theta = 28.6^\circ$ characteristic of ceria cubic phase (JCPDS-4-0593). For the Pt/ $\text{Ce}_{0.75}\text{Zr}_{0.25}\text{O}_2/\text{Al}_2\text{O}_3$ prepared by precipitation (C) and by impregnation (D) there was a shift of this peak from $2\theta = 28.6^\circ$ to 28.8° . The peaks were broader than the one detected for the Pt/ $\text{CeO}_2/\text{Al}_2\text{O}_3$ sample and no diffraction peaks related to the zirconia phases were detected. This observation is consistent with the average particle size based on the peak correspondent to the diffraction of Ce(1 1 1), using the Scherrer equation [36]. For Pt/ $\text{CeO}_2/\text{Al}_2\text{O}_3$ samples, we calculated 164 \AA for the one prepared by precipitation and 140 \AA for the one obtained by impregnation. For ceria–zirconia containing catalysts, the results were 120 \AA for the sample prepared by impregnation and 110 \AA for the precipitated one. Similar results were obtained by Koslov et al. [20] with ceria–zirconia materials (with a Ce/Zr ratio equals to 1) supported on alumina and prepared by co-impregnation and cogellation. According to them, the lower peak intensities verified for ceria–zirconia materials are due to either higher dispersion or a higher degree of disorder of the mixed oxide phase. In this same study the authors suggested, based on the position of the Ce(1 1 1) peak and JCPDS database, that the sample prepared by the cogellation method formed a ceria–zirconia material whose chemical composition was $\text{Ce}_{0.55}\text{Zr}_{0.45}\text{O}_2$. Conversely, the sample prepared by co-impregnation formed a major phase with a ceria–zirconia solid solution ($\text{Ce}_{0.7}\text{Zr}_{0.3}\text{O}_2$) and a minor zirconia rich phase. In our work, we used the methodology proposed by Koslov et al. [20] to calculate the lattice parameter which was based on the position of the reflection Ce(1 1 1) of cubic ceria phase. We could estimate that a

$\text{Ce}_{0.82}\text{Zr}_{0.18}\text{O}_2$ solid solution was formed on the samples prepared by impregnation and precipitation. Although it seems that not all the zirconia was added to the ceria lattice, we could not detect a zirconia rich phase. Notice that in this work the nominal composition for ceria–zirconia material was $\text{Ce}_{0.75}\text{Zr}_{0.25}\text{O}_2$ whereas we obtained a $\text{Ce}_{0.82}\text{Zr}_{0.18}\text{O}_2$ sample according to the position of the Ce(1 1 1) diffraction peak. This means that around 72% of the zirconium added was incorporated to the ceria lattice. On the other hand, for the impregnated sample prepared by Koslov et al. [20] approximately 60% of the zirconium was effectively added to the ceria cubic structure. One possible explanation for this observation is the use of different precursors, Ce^{4+} (from $(\text{NH}_4)_2\text{Ce}(\text{NO}_3)_6$) in this work and Ce^{3+} (from $\text{Ce}(\text{NO}_3)_3$) by Koslov et al. Accordingly to Letichevsky et al. [37], cerium (IV) is present in solution as an anionic complex, while cerium (III) is present as a hydrolyzed cation. This charge difference would benefit the proximity of anionic $\text{Ce}(\text{NO}_3)_6^{2-}$ and the cationic zirconyl (ZrO^{2+}). This process could facilitate the formation of a solid solution.

Table 1 presents the values of the optical density of the band at 1235 cm^{-1} calculated through CO_2 infrared spectra. Accordingly to the literature [38] the optical density of this band can be used as a quantitative measurement of the surface of the alumina that is not covered by ceria or ceria–zirconia. The data showed that the addition of ceria and ceria–zirconia to the alumina led to lower values of optical density independently of the preparation method used, indicating that both methods were effective to disperse the ceria based materials on the surface of the alumina. Comparing Pt/ $\text{Ce}_{0.75}\text{Zr}_{0.25}\text{O}_2/\text{Al}_2\text{O}_3$ prepared by precipitation and by impregnation, it can be noticed that the former had a lower coverage of the alumina than the later. This fact is an indication that during the precipitation, probably islands of ceria–zirconia particles were formed rather than uniformly dispersed on the alumina surface.

The platinum dispersion was evaluated using the dehydrogenation of cyclohexane as a model reaction and the results are presented in Table 1. All the catalysts were within the range of 42 and 48%. Since all the samples were supported on pure alumina or a 14% $\text{CeO}_2/\text{Al}_2\text{O}_3$ and 14% $\text{Ce}_{0.75}\text{Zr}_{0.25}\text{O}_2/\text{Al}_2\text{O}_3$ supports that had BET surface areas around $70 \text{ m}^2/\text{g}$, we did not expect very different values of metal dispersions among the samples. The values of dispersion obtained in this study are higher when compared to the ones obtained for samples supported on bulk ceria and ceria–zirconia materials

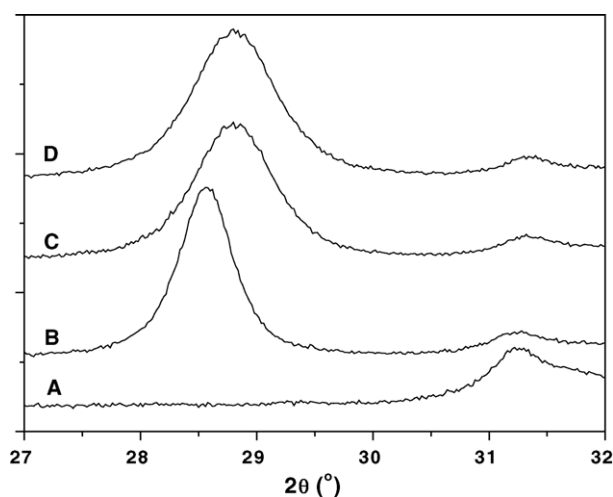


Fig. 2. X-ray diffraction patterns of Pt/ Al_2O_3 (A), Pt/ $\text{CeO}_2/\text{Al}_2\text{O}_3$ (pp) (B), Pt/ $\text{Ce}_{0.75}\text{Zr}_{0.25}\text{O}_2/\text{Al}_2\text{O}_3$ (pp) (C) and Pt/ $\text{Ce}_{0.75}\text{Zr}_{0.25}\text{O}_2/\text{Al}_2\text{O}_3$ (imp) (D). Data collected at 0.02° per step between $2\theta = 27$ and 32° .

Table 1
Optical density of band 1235 cm^{-1} obtained from CO_2 adsorbed infrared and metal dispersions calculated from the cyclohexane dehydrogenation

Samples	Optical density (Alumina)	Platinum dispersion (%)
Pt/ Al_2O_3	25	45
Pt/ $\text{CeO}_2/\text{Al}_2\text{O}_3$ (pp)	17	42
Pt/ $\text{CeO}_2/\text{Al}_2\text{O}_3$ (imp)	2	48
Pt/ $\text{Ce}_{0.75}\text{Zr}_{0.25}\text{O}_2/\text{Al}_2\text{O}_3$ (pp)	20	42
Pt/ $\text{Ce}_{0.75}\text{Zr}_{0.25}\text{O}_2/\text{Al}_2\text{O}_3$ (imp)	16	47

in one of our previous work [16]. The use of the alumina provided a higher surface area, which led to the better metal dispersion.

3.2. Reducibility

The results obtained during oxygen storage capacity measurements are also shown in Table 2. This capacity is associated to the ability of cerium to act as an oxygen buffer by storing/releasing O_2 due to the Ce^{4+}/Ce^{3+} redox couple [22]. The O_2 consumption is significantly higher for ceria–zirconia materials than $Pt/CeO_2/Al_2O_3$ and Pt/Al_2O_3 . These results are in agreement with several studies, which reported that the incorporation of ZrO_2 into CeO_2 lattice promotes the CeO_2 redox properties [32–35].

Fig. 3 presents the temperature programmed reduction profiles of the samples Pt/Al_2O_3 , $Pt/CeO_2/Al_2O_3$ and $Pt/Ce_{0.75}Zr_{0.25}O_2/Al_2O_3$ prepared by impregnation and precipitation. The Pt/Al_2O_3 catalyst had only a reduction peak around 500 K that can be attributed to the reduction of $PtCl_xO_y$ [39]. The $Pt/CeO_2/Al_2O_3$ sample prepared by impregnation presented H_2 consumption peaks at 383, 433 and 1063 K, while $Pt/CeO_2/Al_2O_3$ prepared by precipitation showed peaks at higher temperatures (423, 493 and 1213 K). These results are in agreement with the ones obtained by Yao and Yao [40] that studied $Pt/CeO_2/Al_2O_3$ and observed reduction peaks between 423 and 650 K. Accordingly to them, the reduction peaks at lower temperatures can be ascribed to the reduction of platinum oxide and to the reduction of cerium oxide that was promoted by the metal. Both samples also had high temperature peaks, which can be attributed to the reduction of ceria that was not promoted by the metal. These high temperature peaks are usually ascribed to the formation of $CeAlO_3$ that occurs after the complete reduction of small ceria particles and to the formation of Ce_2O_3 coming from the bulk ceria particles [21,41–43].

Both $Pt/Ce_{0.75}Zr_{0.25}O_2/Al_2O_3$ samples showed high temperature reduction peaks around 1123 K with intensities

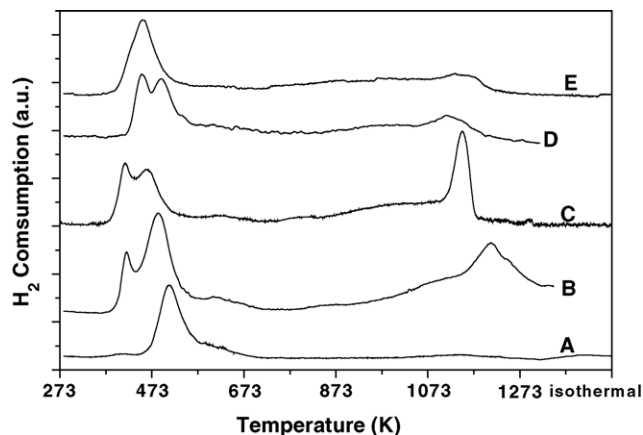


Fig. 3. Temperature programmed reduction profiles of Pt/Al_2O_3 (A), $Pt/CeO_2/Al_2O_3$ (pp) (B), $Pt/CeO_2/Al_2O_3$ (imp) (C), $Pt/Ce_{0.75}Zr_{0.25}O_2/Al_2O_3$ (pp) (D) and $Pt/Ce_{0.75}Zr_{0.25}O_2/Al_2O_3$ (imp) (E).

Table 2
Oxygen storage capacities and temperature programmed reduction results

Samples	O_2 consumption ($\mu\text{mol/g}_{\text{cat}}$)	Total H_2 consumption ($\mu\text{mol/g}_{\text{cat}}$)	H_2 consumption below 873 K ($\mu\text{mol/g}_{\text{cat}}$)
Pt/Al_2O_3	0	82	82
$Pt/CeO_2/Al_2O_3$ (pp)	63	352	157
$Pt/CeO_2/Al_2O_3$ (imp)	391	313	129
$Pt/Ce_{0.75}Zr_{0.25}O_2/Al_2O_3$ (pp)	215	166	97
$Pt/Ce_{0.75}Zr_{0.25}O_2/Al_2O_3$ (imp)	179	221	157

much lower than the ones obtained for $Pt/CeO_2/Al_2O_3$ samples. The majority of the H_2 consumption occurred at low temperature between 423 and 673 K. This consumption is ascribed to both the reduction of the $PtCl_xO_y$ and to the partial reduction of cerium oxide promoted by Pt. This decrease in the reduction temperature when comparing ceria–zirconia materials with ceria based samples is well described in the literature and it is due to the addition of zirconium to ceria lattice, which increases ceria reducibility [16,30,33]. The presence of zirconium promotes the oxygen mobility leading to easy formation of oxygen vacancies. For the $Pt/Ce_{0.75}Zr_{0.25}O_2/Al_2O_3$ (imp), the total H_2 consumption was around 25% higher than the one observed for the same sample prepared by precipitation. In addition, the H_2 consumption below 873 K represents 71% of the total for the sample prepared by impregnation, while for the one obtained by precipitation, this consumption corresponded to only 58% of the total. This result is in agreement with the infrared results that show a better dispersion of the ceria–zirconia on the samples prepared by impregnation. Since all the samples have similar platinum dispersions, there is probably a better interaction between platinum and ceria for the samples obtained by impregnation.

3.3. Methane partial oxidation

Figs. 4–7 show the activity and selectivity results of all samples during the 24 h reaction period. All the samples exhibited approximately the same initial conversion, which agrees very well with the similar dispersion of these catalysts. The only exception is the $Pt/CeO_2/Al_2O_3$ catalyst that was slightly more active than the other catalysts. The samples prepared by impregnation were quite stable, while the others prepared by precipitation and the Pt/Al_2O_3 sample deactivated strongly and after the 24 h period presented a methane conversion around 20%.

The selectivity for H_2 formation for the samples prepared by impregnation was around 90% and was practically constant over the 24 h reaction period (Fig. 5). On the other hand, for the Pt/Al_2O_3 and the samples prepared by precipitation, a strong decrease on the H_2 formation was detected after 4 h of reaction.

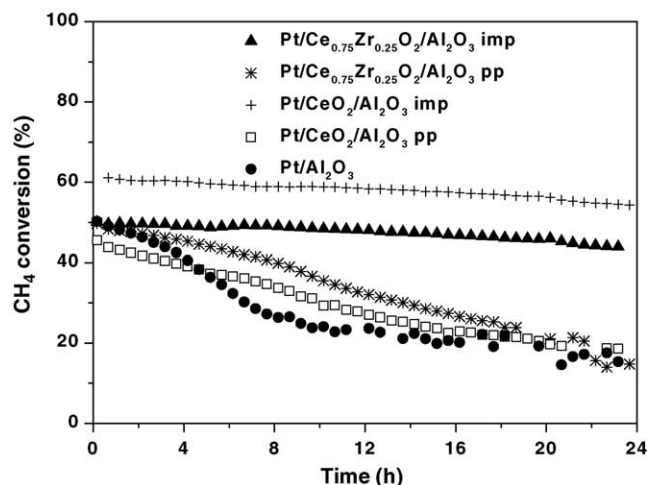


Fig. 4. CH_4 conversion during 24 h of methane partial oxidation $T_{\text{reaction}} = 1073 \text{ K}$ and $\text{WHSV} = 260 \text{ h}^{-1}$.

The CO selectivity was practically constant on the catalysts prepared by impregnation whereas it strongly decreased as a function of TOS on $\text{Pt}/\text{Al}_2\text{O}_3$ and catalysts obtained by precipitation. The selectivity for CO_2 formation presented an opposite behavior: at the beginning of the reaction period it was low for all samples. However, while for the catalysts prepared by impregnation the value was approximately stable around 20%, for all the other samples, it started around 25% and increased to 65–70% after 24 h.

Even though there are studies in the literature about ceria–zirconia samples supported on alumina, we could not find any report about the use of these systems for methane partial oxidation. For this reason, the discussion of the results will be done by comparison of the samples of this work with platinum supported on bulk ceria–zirconia materials. In a previous report, Mattos et al. [16] observed the same behavior while studying $\text{Pt}/\text{Al}_2\text{O}_3$, Pt/ZrO_2 , and $\text{Pt}/\text{Ce}_{0.75}\text{Zr}_{0.25}\text{O}_2$. The first two samples deactivated strongly, while the catalyst supported

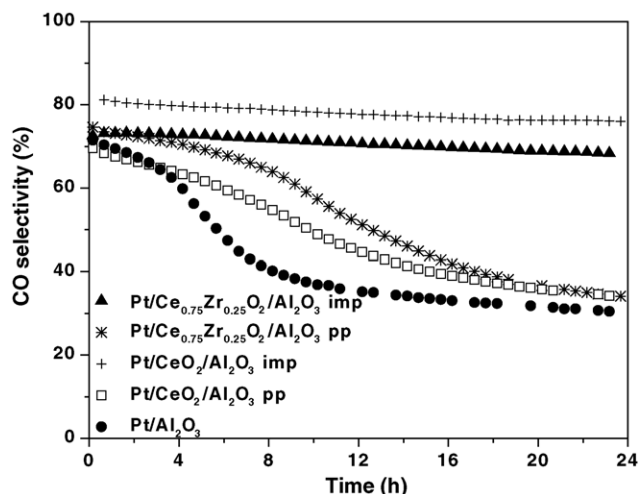


Fig. 6. CO selectivity during 24 h of methane partial oxidation $T_{\text{reaction}} = 1073 \text{ K}$ and $\text{WHSV} = 260 \text{ h}^{-1}$.

on ceria–zirconia remained stable and with high H_2 and CO selectivities during 24 h. For the catalysts prepared by precipitation and $\text{Pt}/\text{Al}_2\text{O}_3$ in this work, as the activity decreased, the CO_2 selectivity increased and H_2 and CO selectivities decreased. The same result was reported by Mattos et al. [16] for $\text{Pt}/\text{Al}_2\text{O}_3$ and Pt/ZrO_2 samples. These results were explained taking into account the two steps mechanism of the partial oxidation of methane. In the first step of this mechanism, methane would go through total oxidation forming CO_2 and H_2O . In the second step, unreacted methane would be reformed by CO_2 and H_2O producing CO and H_2 . Based on this mechanism, the authors concluded that the second step of the mechanism was inhibited on $\text{Pt}/\text{Al}_2\text{O}_3$ and Pt/ZrO_2 samples since the production of CO_2 increased.

According to the mechanism of the CO_2 reforming of methane [44], the support participates in the dissociative adsorption of CO_2 . This mechanism proposes that the support supplies oxygen to the metal surface, promoting the

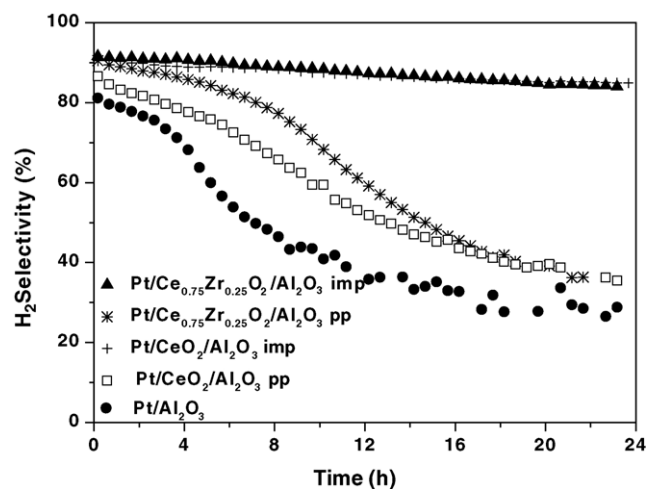


Fig. 5. H_2 selectivity during 24 h of methane partial oxidation $T_{\text{reaction}} = 1073 \text{ K}$ and $\text{WHSV} = 260 \text{ h}^{-1}$.

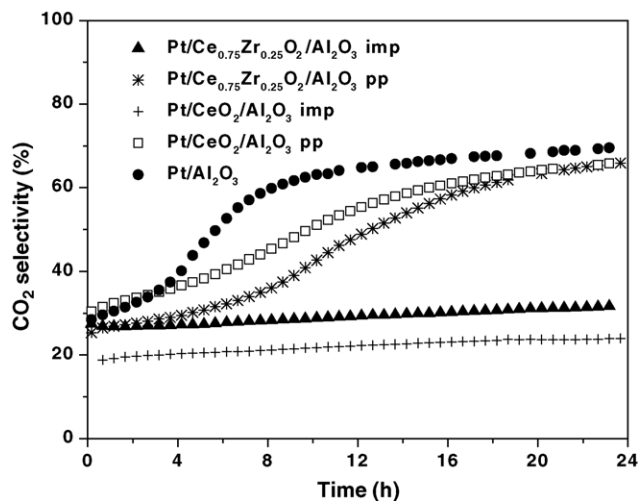


Fig. 7. CO_2 selectivity during 24 h of methane partial oxidation $T_{\text{reaction}} = 1073 \text{ K}$ and $\text{WHSV} = 260 \text{ h}^{-1}$.

removal of carbon deposited on the metal. Then, a high metal–support interfacial area is fundamental for efficient cleaning of the metal particle.

Therefore, in this work, the strong deactivation observed on the Pt/Al₂O₃ and on the samples prepared by precipitation could be attributed to the formation of carbon deposits on the metal surface, due to the absence of an effective cleaning mechanism of the support. In the case of Pt/CeO₂/Al₂O₃ (pp) and Pt/Ce_{0.75}Zr_{0.25}O₂/Al₂O₃ (pp) catalysts, this result is quite surprising since both catalysts presented oxygen storage capacity similar to the ones prepared by impregnation. Furthermore, it can be noticed that all the samples had practically the same metal dispersion. However, the coverage degree of alumina on the precipitated catalysts was much lower than that on the catalysts prepared by impregnation. It means that a larger fraction of platinum particles is deposited over alumina and it is not in contact with ceria–zirconia oxide. The metal–support interface is a key factor to avoid the carbon deposits that are responsible for the deactivation of some samples. Furthermore, these results reveal that the preparation method has a crucial role on the performance of the catalysts. The preparation method that favors a high coverage degree of the alumina by the ceria-based oxide promotes the presence of an efficient cleaning mechanism of the metal particle and then, inhibits the deactivation of the catalyst.

4. Conclusions

The impregnation method was more effective to disperse the ceria based materials on the surface of the alumina than the precipitation method. All the samples had the same metal dispersion and the use of alumina provided a higher exposed metal surface than when bulk ceria materials are used. The catalysts prepared by impregnation had higher percentage of the alumina covered by ceria or ceria–zirconia than the ones prepared by precipitation. This probably resulted on higher metal and ceria interaction for these samples, which may be responsible for the higher stability and better CO and H₂ selectivities on the methane partial oxidation observed for these catalysts.

Acknowledgements

The authors wish to acknowledge the financial support of the CAPES and CNPq. We also thank MEL Chemicals for providing the zirconium hydroxide.

References

- [1] J.R. Rostrup-Nielsen, Catal. Today 63 (2000) 159.
- [2] T. Zhu, M. Flytzani-Stephanopoulos, Appl. Catal. A: Gen. 208 (2001) 403.
- [3] V.R. Choudhary, A.M. Rajput, B. Prabhakar, A.S. Mamman, Fuel 77 (15) (1998) 1803.
- [4] I. Dykkjaer, T.S. Christensen, Stud. Surf. Sci. Catal. 136 (2001) 435.
- [5] Y.H. Hu, E. Ruckenstein, J. Catal. 158 (1996) 260.
- [6] P.D.F. Vernon, M.L.H. Green, A.K. Cheetham, A.T. Ashcroft, Catal. Lett. 6 (1990) 181.
- [7] D.A. Hickman, L.D. Schmidt, Science 259 (1993) 343.
- [8] D.A. Hickman, E.A. Haupfear, L.D. Schmidt, Catal. Lett. 17 (1993) 223.
- [9] J.H. Lunsford, Catal. Today 63 (2000) 165.
- [10] D.B. Bukur, X. Lang, Y. Ding, Appl. Catal. A: Gen. 186 (1999) 255.
- [11] L. Basini, A. Guarinoni, A. Aragno, J. Catal. 190 (2000) 284.
- [12] V.R. Choudhary, A.S. Mamman, Fuel Process. Technol. 60 (3) (1999) 203.
- [13] C.H. Au, C.F. Ng, M.S. Liao, J. Catal. 185 (1999) 12.
- [14] S.C. Tsang, J.B. Claridge, M.L.H. Green, Catal. Today 23 (1995) 3.
- [15] W.S. Dong, H.S. Roh, K.W. Jun, S.E. Park, Y.S. Oh, Appl. Catal. A: Gen. 226 (2002) 63.
- [16] L.V. Mattos, E.R. De Oliveira, P.D. Resende, F.B. Noronha, F.B. Passos, Catal. Today 77 (2002) 245.
- [17] K. Otsuka, Y. Wang, E. Sunada, I. Yamanaka, J. Catal. 175 (1998) 152.
- [18] P. Pantu, K. Kim, G.R. Gavalas, Appl. Catal. A: Gen. 193 (1–2) (2000) 203.
- [19] M. Fernández-García, A. Martínez-Arias, A. Iglezias-Juez, C. Belver, A.B. Hungria, J.C. Conesa, J. Soria, Appl. Catal. B: Environ. 31 (2001) 39.
- [20] A.I. Koslov, D.H. Kim, A. Yezerets, Y. Andersen, H.H. Kung, M.C. Kung, Catal. Today 75 (2002) 401.
- [21] M. Fernández-García, A. Martínez-Arias, A. Iglezias-Juez, C. Belver, A.B. Hungria, J.C. Conesa, J. Soria, J. Catal. 194 (2000) 385.
- [22] M.H. Yao, R.J. Baird, F.W. Kunz, T.E. Hoost, J. Catal. 166 (1997) 67.
- [23] A. Iglesias-Juez, A. Martínez-Arias, M. Fernández-García, J. Catal. 221 (2004) 148.
- [24] J.G. Nunan, W.B. Williamson, W.J. Robota, SAE Paper 960798, 1996.
- [25] R. Di Monte, P. Fornasiero, J. Kaspar, P. Rumori, G. Gubitosa, M. Graziani, Appl. Catal. B: Environ. 24 (2000) 157.
- [26] E. Rogemond, N. Essayem, R. Fréty, V. Perrichon, M. Primet, F. Mathis, J. Catal. 166 (1997) 229.
- [27] P. Pantu, G. Gavalas, Appl. Catal. A: Gen. 223 (2002) 253.
- [28] C. Carnevillier, F. Epron, P. Marecot, Appl. Catal. A: Gen. 275 (1–2) (2004) 25–33.
- [29] Y.K. Park, F.H. Ribeiro, G.A. Samorjai, J. Catal. 178 (1998) 66.
- [30] L. Pino, V. Recupero, S. Beninati, A.K. Shukla, M.S. Hegde, P. Bera, Appl. Catal. A: Gen. 225 (2002) 63.
- [31] S.M. Stagg-Williams, F.B. Noronha, Recent Research Developments in Catalysis, vol. 2, 2003, pp. 205–230 Chapter 10.
- [32] T. Murota, T. Hasegawa, S. Aozasa, H. Matsui, M. Motoyama, J. Alloys Comp. 193 (1993) 298.
- [33] C. de Leitenburg, A. Trovarelli, J. Llorca, F. Cavani, G. Bini, Appl. Catal. A: Gen. 139 (1996) 161.
- [34] A. Trovarelli, F. Zamar, J. Llorca, C. de Leitenburg, G. Dolcetti, J.T. Kiss, J. Catal. 169 (1997) 490.
- [35] C.E. Hori, H. Permana, K.Y. Ng Simon, A. Brenner, K. More, K.M. Rahmoeller, D. Belton, Appl. Catal. B: Environ. 16 (1998) 105.
- [36] H.P. Klug, L.E. Alexander, X-ray Diffraction Procedures for Polycrystalline Amorphous Materials, Wiley, New York, 1974.
- [37] S. Letichevsky, C.A. Tellez, R.R. de Aveliz, M.I.P. da Silva, M.A. Fraga, L.G. Appel, Appl. Catal. B: Environ., submitted for publication.
- [38] R. Fréty, P.J. Lévy, V. Perrichon, V. Pitchon, M. Primet, E. Rogemond, N. Essayem, M. Chevrier, C. Gauthier, F. Mathis, Stud. Surf. Sci. Catal. 96 (1995) 405.
- [39] D.A.G. Aranda, F.B. Noronha, M. Schmal, F.B. Passos, Catal. Appl. A: Gen. 100 (1993) 77.
- [40] H.C. Yao, Y.F.Y. Yao, J. Catal. 86 (1984) 254.
- [41] S. Damyanova, J.M.C. Bueno, Appl. Catal. A: Gen. 253 (2003) 135.
- [42] J.Z. Shyu, W.H. Weber, H.S. Gandhi, J. Phys. Chem. 92 (1988) 4964.
- [43] R.L. Monteiro, F.B. Noronha, L.C. Dieguez, M. Schmal, Appl. Catal. A: Gen. 131 (1995) 89.
- [44] S.M. Stagg-Williams, F.B. Noronha, G. Fendley, D.E. Resasco, J. Catal. 194 (2000) 240.